

Optical Flow Methods for PUNCH Imaging

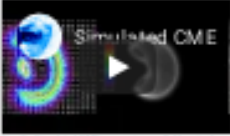
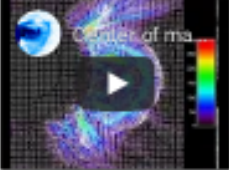


Optical Flow Methods for PUNCH Imaging

Robin Colaninno and Phil Hess

U.S. Naval Research Laboratory



Background	Application of Optical Flow	LASC0 Results	Application to PUNCH
<p>Optical Flow Technique</p> <p>Optical flow is the vector field that maps one image into another [1]. If the two images are of the same scene separated by some time Δt, then these vectors can be interpreted as the motion of the scene. The optical flow is the 2D projection of the 3D motion of the observed scene. The definition of optical flow can be written mathematically as:</p> $\vec{f}(s) + \Delta t \vec{w}_s \cdot \nabla - \Delta I(s, t) = 0$ <p>Where \vec{w} is the vector that maps the image $I(s, t)$ into the image $I(s, t + \Delta t)$. Equation (1) is nonlinear and requires the unknown velocity vector. The optical flow constraint equation is the horizontal component of equation (1):</p> $\nabla_x I(s, t) \cdot \vec{w}_s + f_x(s, t) = 0$ <p>Where ∇_x is the spatial gradient across x and f_x is the frame-to-frame difference.</p> <p>Equation (2) is ill-posed and does not allow us to solve for the velocity vector from the scalar intensity. To constrain the solution, we add a smoothness regularization term. We can then express the minimization of the optical flow as a global energy minimization [2]. The energy function we minimize is:</p> $E(\vec{w}_s, f) = \sum (\nabla_x I(s, t) \cdot \vec{w}_s + f_x(s, t))^2$ <p style="text-align: center;">OPEN</p>	<p>Previous Methodology</p> <p>We have previously applied the optical flow technique to 30-day LASC0 C2 CME sequences. We first reduced the technique on a simulated CME sequence [3]. For the test CMEs we studied, we found that the measured optical flow velocity of the bubble did not vary from the LASC0-CME Catalog (4) velocity by more than 20% [4]. Figure 2 and 3 show the individual and combined frame images and the optical flow results. The coloring represents the velocity magnitude. The arrows show the direction of the velocity. The scale bar is in km/s.</p> <p>Simulated CME</p>  <p>Fig. 2. Simulated CME - mean image (left) optical flow results (right).</p> <p>We used calculated mean images to avoid the effects of Thomson scattering. The projected front velocity of the CME is calculated in km/s. You can see that we are achieving this velocity over the front of the CME. Inside the CME, where the intensity is not changing, there is no calculated velocity though we know there is motion there. This is an effect of the constant intensity of the simulated CME.</p> <p style="text-align: center;">OPEN</p>	<p>Link and to remote Velocity</p> <p>Optical flow highlights the velocity of velocities in different parts of the CME. The vector field highlights sections that are not part of the CME front.</p>  <p>Fig. 4. The bulk motion of the CME has been removed from the motion of the LASC0 C2 1 September 2012 CME. The mean highlights the respective velocity of the CME.</p> <p>We used a simple model to define the bulk and respective velocity of the CME. If the CME is an expanding bubble moving away from the sun, then translation of the bubble from the Sun to the bulk speed and the expansion of the bubble is the respective speed. To approximate the expansion and bulk speeds from the vector field, we first find the centers in the CME optical flow field that are completely vertical or completely horizontal in the reference frame of the image. In Figures 5 and 6, these points are shown as white dots. We then fit:</p> <p style="text-align: center;">OPEN</p>	<p>Optical Flow with PUNCH</p> <p>One of the main goals of the PUNCH mission is to produce velocity flow maps of the solar corona from 6 to 30 R_sun. PUNCH will produce data at a higher cadence (> 8 minutes) than the previous applications to LASC0 C2. The goal of PUNCH is to determine the velocity of both the solar wind and CMEs.</p> <p>The optical flow method presented here has been proven to work on CMEs in LASC0 C2 data. The method has several advantages that makes it a good candidate for PUNCH:</p> <ul style="list-style-type: none"> • Direct field... creates an estimate of the velocity steering point. To estimate the solar wind flow a direct field of velocity vectors is required. Many methods do not create a direct field of velocity estimates. • Robustness... highly robust to image noise. Performance is comparable to the previous state of central observations such as the solar field and the superposition of optically thin plasma. • Starting assumptions... does not require a priori assumptions to determine velocity field. Some methods require an estimate of the velocity to begin the minimization. In contrast a prior estimate can bias the determination of the true velocity. <p>Other Methods</p> <p>There are a large variety of ways to solve the optical flow problem. One of the first papers to compare different optical flow techniques is Horn, Hough and Brodatz (1986). The authors consistently compare different techniques to the same dataset. Current state of the art algorithms are evaluated as:</p> <p style="text-align: center;">OPEN</p>

[AUTHOR INFORMATION](#) [ABSTRACT](#) [REFERENCES](#) [CONTACT AUTHOR](#) [PRINT](#) [GET POSTER](#)

Robin Colaninno and Phil Hess

U.S. Naval Research Laboratory



PRESENTED AT:



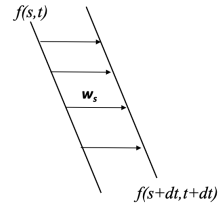
AGU FALL MEETING

Online Everywhere | 1-17 December 2020

BACKGROUND

Optical Flow Technique

Optical flow is the vector field that warps one image into another [1]. If the two images are of the same scene separated by some time dt , then these vectors can be interpreted as velocities. These vectors are the 2D projection of the true 3D motion of the observed scene. The definition of optical flow can be written analytically as:



$$f(s+dt \mathbf{w}_s, t+dt) - f(s, t) \approx 0 \quad (1)$$

Where \mathbf{w}_s is the vector that warps the image $f(s, t)$ into the image $f(s+dt, t+dt)$. However, equation (1) is nonlinear with respect to the unknown velocity vector. The optical flow constraint equation is the linearized expansion of equation (1),

$$\nabla f(s, t) \cdot \mathbf{w}_s + f_t(s, t) \approx 0 \quad (2)$$

Where ∇f is the spatial gradient at time t and f_t is the frame-to-frame difference.

Equation (2) is *ill posed* and does not allow us to solve for the velocity vector from the scalar intensity. To constrain the solutions, we add a smoothness regularization term. We can then express the estimation of the optical flow as a global energy minimization [2]. The energy function we minimize is:

$$H(\mathbf{w}; f) = \sum_{s \in S} [\nabla f(s, t) \cdot \mathbf{w}_s + f_t(s, t)]^2 + \alpha \sum_{(s,r) \in C} \|\mathbf{w}_s + \mathbf{w}_r\|^2 \quad (3)$$

Where the first term is optical flow estimation and the second is the smoothing regularization MRF over neighboring site pairs \mathbf{w}_r .

Limitations

Equation (2) is a very simple interpretation of the motion in a scene. It relies solely on changes in intensity to estimate the motion. It assumes that any change in intensity is caused by motion and not an intrinsic change in brightness. This assumption limits the accuracy of the optical flow estimation of a CME which has intrinsic brightness variations.

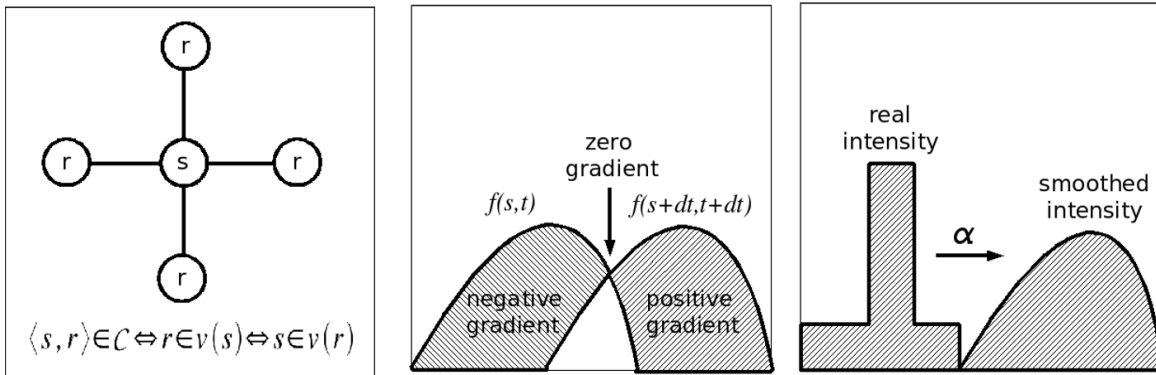


Fig. 1 - Illustrates some limitations of the optical flow method. (LEFT) The formulation requires that temporal and spatial are on the order of the regularization neighborhood. (CENTER) The optical flow assumption is easily violated especially in regions without intensity variations. (RIGHT) The assumption that the velocity varies smoothly is often violated at the front edge of the CME.

There are other limitations to this method inherent to the formulation. It assumes that the temporal and spatial changes are small. This assumption imposes an artificial upper speed limit to the technique. The next limitations come from the easily violated optical flow assumptions. If there is a place in the image where there is motion but no change in intensity the program does not calculate a velocity. We see this in particular in the coronal images where the front intersects in two consecutive images. The addition of the regularization assumes the velocity field varies smoothly which is not true at edges. This is a pretty good assumption for motion in the corona but not in all cases. Unfortunately, all these limitations combined to reduce the magnitude of the calculated velocity.

APPLICATION OF OPTICAL FLOW

Previous Application

We have previously applied this optical flow technique to SOHO LASCO C2 CME sequences. We first validated the technique on a simulated CME sequence [3]. For the ten CMEs we studied, we found that the estimated optical flow velocity of the front did not vary from the LASCO CME Catalog HT velocity by more than 30% [4]. Figure 2 and 3 show the calculated and observed mass images and the optical flow results. The coloring represents the velocity magnitude. The arrows show the direction of the velocity. The scale bar is in km/s.

Simulated CME

[VIDEO] <https://www.youtube.com/embed/2K9yabHHV1Q?rel=0&fs=1&modestbranding=1&rel=0&showinfo=0>

Fig. 2 - Simulated CME - mass image (left) optical flow results (right).

We used calculated mass images do avoid the effects of Thomson scattering. The projected front velocity of the CME simulation is 300 km/s. You can see that we are achieving this velocity near the front of the CME. Interior to the CME, where the intensity is not changing there is no calculated velocity though we know there is motion there. This is an artifact of the constant intensity of the simulated CME.

LASCO CME on 2002 September 1

[VIDEO] <https://www.youtube.com/embed/jDJ6WKZX5TU?rel=0&fs=1&modestbranding=1&rel=0&showinfo=0>

Fig. 3 - LASCO CME on 2002 September 1 - mass image (left) optical flow results (right).

We applied our method to a CME observed in LASCO C2. The measured front velocity for this event was 230km/s. Again, we are able to capture a representative front velocity, as well as, velocity throughout the CME. We also find the velocity of the streamer deflection above the CME.

LASCO RESULTS

Bulk and Expansion Velocity

Optical flow highlights the variety of velocities in different parts of the CME. The vector field highlights motions that are not part of the CME front.

[VIDEO] <https://www.youtube.com/embed/TXB1ETtBsBk?rel=0&fs=1&modestbranding=1&rel=0&showinfo=0>

Fig. 4 - The bulk motion of the CME has been removed from the motion of the LASCO C2 1 September 2002 CME. The movie highlights the expansion velocity of the CME.

We used a simple model to define the bulk and expansion velocity of the CME. If the CME is an expanding bubble moving away from the sun, then translation of the bubble from the Sun is the bulk speed and the expansion of the bubble is the expansion speed. To separate the expansion and bulk speeds from the vector field, we first find the vectors in the CME optical flow field that are completely vertical or completely horizontal in the reference frame of the image. In Figures 5 and 6, those points are shown as white dots. We then fit the two solid lines to these points. The intersection of the solid lines is defined as center of motion. Next, we then fit a line to the point in each quadrant separately. These fits are shown as the dashed lines in Figures 5 and 6. We use the distance from the center of motion to the dashed lines as the expansion. The selection of the points and fitting of the lines is all done automatically.

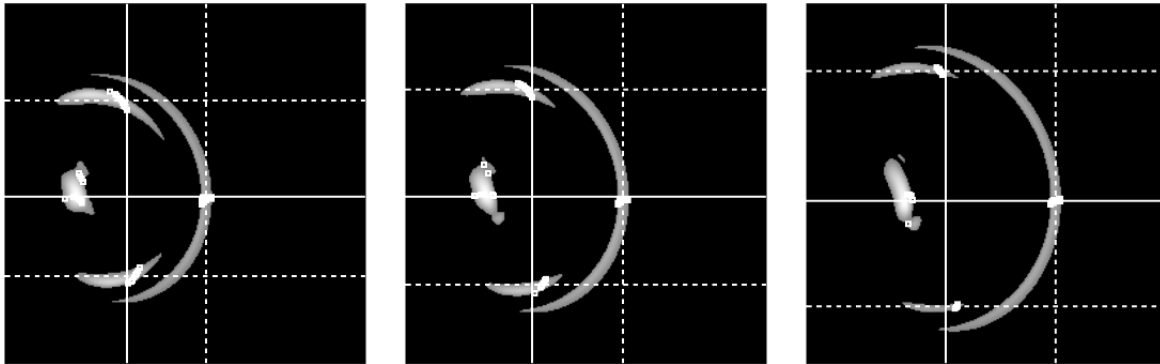


Fig. 5 - Example of the selection of the bulk and expansion velocities for three different times of the simulated CME.

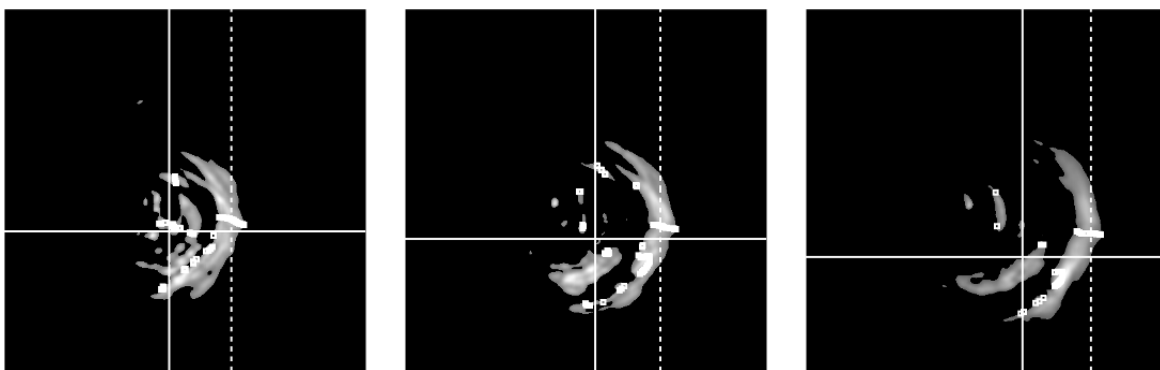


Fig. 6 - Example of the selection of the bulk and expansion velocities for three different times of the LASCO 1 September 2020 CME. The expansion of the CME flanks is not detected using this method.

Height-Time Plots

We used the bulk and expansion values extracted from the optical flow maps to make a height-time plots for all of these points. For the simulated CME, we were able to measure the expansion in three direction. For the LASCO CME, we could only measure the leading edge. Our results from our numeric approach show that the position angel of the center of motion is the same as the

user chosen position angle from the catalog. By adding the bulk and expansion velocity, we get approximately the front velocity. Given our model of the expanding translating bubble, this is what we expected.

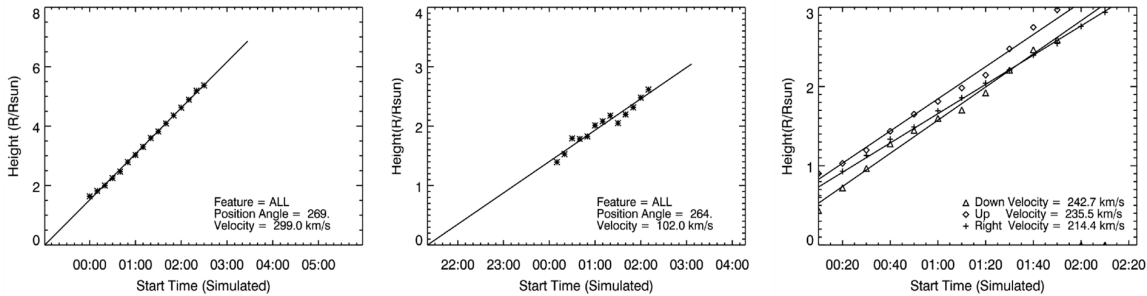


Fig. 7 - (LEFT) The front of the simulated CME is at a known position at each time step. (CENTER) The height is the center of motion. The linear fit of this height-time plot gives a bulk velocity for the CME. (RIGHT) The distance from the center of motion to the right, top and bottom of the CME. From this plot, we get the expansion velocity in three directions.

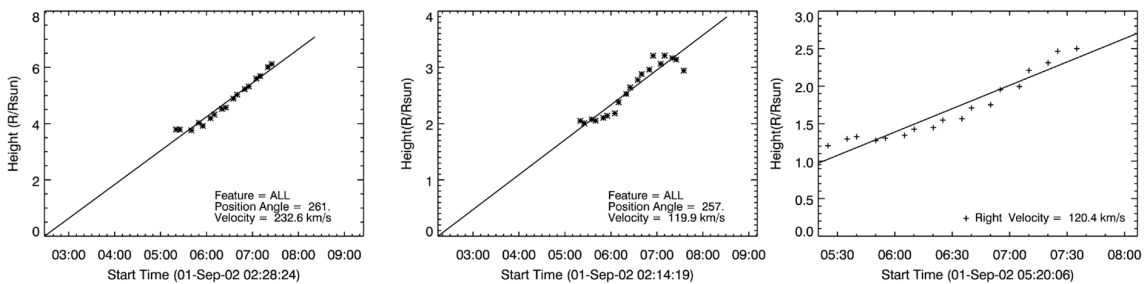


Fig. 8 - (LEFT) The CME front heights from the CDAW SOHO LASCO CME Catalog [5]. (CENTER) The height is the center of motion. The linear fit of this height-time plot gives a bulk velocity for the CME. (RIGHT) The distance of the front from the center of motion. From this plot, we get the expansion velocity.

We applied our optical flow method to 10 CMES observed in LASCO C2. We are limited in the CMES that we can apply our method to because of the limitation of small motions frame-to-frame. The nominal time cadence of LASCO C2 observations is too high for average CME speeds. We analyzed periods during the mission when the cadence was increased to 10 or 12 minutes. Also, we must look at velocities below 300 km/s in the LASCO C2 FOV. In the table below, most of the average front velocities from the optical flow are less than the CDAW height-time velocity from the catalog. The optical flow derived velocities do not vary from the catalog velocity by more than 30%. The position angle is in better agreement with the catalog values. For most of the CMES we looked at we were able to separate the bulk and expansion. We could not apply it to all the CMES because not all our CME fit our expanding bubble model.

TABLE 1
CME FRONT VELOCITY

CME	Time	HT (km s ⁻¹)	HT PA (deg)	AOF (km s ⁻¹)	Bulk PA (deg)	Bulk Velocity (km s ⁻¹)	Expansion Velocity (km s ⁻¹)
Simulated	299	269	218	264	109	204
2000 Jun 18	18:50	233	262	166	264	43	177
2001 Feb 20	17:00	202	301	236	288	94	100
2001 May 13	12:20	273	234	191	228	123	120
2002 Jan 13	07:35	215	55	184	53	152	76
2002 Apr 2	15:35	152	88	132	84
2002 Sep 1	04:35	233	261	204	257	120	120
2002 Sep 1	19:40	215	30	191	30	72	106
2003 Sep 28	13:00	220	138	167	142
2004 Jun 26	07:48	211	85	216	83	155	18
2004 Jun 27	09:12	220	299	185	298	148	93

NOTES.—CME time is the time of the first appearance of the CME in the LASCO C2 field of view. HT is the front speed derived by a standard height time plot. The AOF (average optical flow) is describe in § 3.2. HT PA, and bulk PA are the position angles of the CME front and center of motion, respectively. The bulk and expansion velocities are described in § 4. The structures of the CMES at 2002 Apr 2 15 : 35 and 2003 Sep 28 13 : 00 do not conform with the model used to measure the bulk and expansion velocities.

^a HT velocity calculated using only LASCO C2 data.

Results from Colaninno, R.C. & Vourlidas, A., 2006, The Astrophysical Journal, 652 : 1747-1754.

APPLICATION TO PUNCH

Optical Flow with PUNCH

One of the science goals of the PUNCH mission is to produce velocity flow maps of the entire corona from 6 to 180 R_{\odot} . PUNCH will produce data at a higher cadence (< 8 minute) than the previous application to LASCO C2. The goal of PUNCH is to determine the velocity of both the solar wind and CMEs.

The optical flow method presented here has been proven to work on CMEs in LASCO C2 data. The method has several advantages that makes it a good candidate for PUNCH.

- Dense field – creates an estimate of the velocity at every pixel. To estimate the solar wind flow a dense field of velocity vectors is required. Many methods do not create dense field of velocity estimates.
- Robustness – highly robust to image noise. Robustness is important due to the intrinsic noise of coronal observations such as the star field and the superposition of optically thin plasma.
- Starting assumptions – does not require a priori assumptions to determine velocity field. Some methods require an estimate of the velocity to begin the minimization. Inaccurate a priori estimates can bias the determination of the true velocity.

Other Methods

There are a large variety of ways to solve the optical flow problem. One of first papers to compare different optical flow techniques is Barron, Fleet and Beauchemin (1994). The authors consistently compare different techniques to the same dataset. Current state-of-the-art algorithms are evaluated on the Middlebury Benchmark Dataset [6]. Older implementations are often explicitly derived from first principles and can be easier to understand. Many of the state-of-the-art techniques are optimized for specific applications that are not similar to coronal observations. The technique that we applied to LASCO is a modification of the Horn and Schunck (1984) method. There are a several other techniques that relied on the spatiotemporal derivative of the optical constraint equation (1). Other techniques are region-based matching such as cross-correlation. Or energy-based methods that work in the Fourier domain. Or more complicated phase-based techniques that combine multiple step analysis of the scene.

Differential Techniques – spatiotemporal derivatives

- Horn and Schunck – gradient constraint equation with global smoothness
- Lucas and Kanade – weighted least-squares fit of local first-order constraints
- Nagel – second-order derivatives with global smoothness constraint
- Uras, Giroso, Verri and Torre – second-order based on a local solution

Region-Based Matching – cross-correlation or sum-of-squared difference (SSD)

- Anandan – Laplacian pyramid and a coarse-to-fine SSD-base matching
- Singh – two-stage matching method 1) SSD and 2) neighborhood constraints

Energy-Based Methods – frequency-based methods in the Fourier domain

- Heeger – least-squares fit of spatiotemporal energy to a plane in frequency space

Phase-Based Techniques - phase behavior of band-pass filters

- Waxman, Wu and Bergholm – spatiotemporal filters to binary maps to track edges
- Fleet and Jepson – instantaneous motion normal to level phase contours in the output of band-pass velocity-tuned filters

AUTHOR INFORMATION

Robin C. Colaninno

Astrophysicist

U.S. Naval Research Laboratory

Washington, DC 20375

Space Science Division

robin.colaninno@nrl.navy.mil

Dr. Colaninno is the Lead of NFI coronagraph for the NASA mission PUNCH, scheduled for launch in 2023. She is PI of SoloHI for ESA Solar Orbiter and a Co-I for NASA Parker Solar Probe WISPR. Dr. Colaninno has more than 15 years of experience analyzing CMEs in coronagraphic and heliographic imaging data. She has developed and published multiple techniques for deriving physical parameter of CMEs from observations. She was the lead developer of the calibration software for the STEREO/SECCHI instrument suite.

Employment:

2012 – current Astrophysicist, Solar & Heliospheric Physics Branch

U.S. Naval Research Laboratory, Washington, DC

2009 – 2012 SCEP Student, Solar Physics Branch

U.S. Naval Research Laboratory, Washington, DC

2006 – 2009 Research Assistant at U.S. Naval Research Laboratory

George Mason University, Fairfax, VA

2003 – 2006 Research Assistant at U.S. Naval Research Laboratory

The Catholic University of America, Washington, DC

Education:

2005 – 2012 Physics PhD. George Mason University, Fairfax, VA

1999 – 2002 Physics B.S. Guilford College, Greensboro, NC

Awards:

Annual Research Publication Award Dinner, 2020 US Naval Research Laboratory

Award of Merit for Group Achievement, 2019 US Naval Research Laboratory

Selected Publications:

R. A. Howard, A. Vourlidas, R. C. Colaninno, C. M. Korendyke, S. P. Plunkett, M. T. Carter, D. Wang, N. Rich, S. Lynch, A. Thurn, D. G. Socker, A. F. Thernisien, D. Chua, et al., “The Solar Orbiter Heliospheric Imager (SoloHI),” A&A, accepted May 2019.

F. Auchère, V. Andretta, E. Antonucci, N. Bach, M. Battaglia, A. Bemporad, D. Berghmans, E. Buchlin, S. Caminade, M. Carlsson, J. Carlyle, J. J. Cerullo, P. C. Chamberlin, R. C. Colaninno, et al., “Coordination within the remote sensing payload on the Solar Orbiter mission,” *A&A*, accepted Jan. 2020.

P. Hess, A. P. Rouillard, A. Kouloumvakos, P. C. Liewer, J. Zhang, S. Dhakal, G. Stenborg, R. C. Colaninno, and R. A. Howard, “WISPR Imaging of a Pristine CME,” *ApJS* 246 (Feb., 2020) 25-26.

R. A. Howard, A. Vourlidas, V. Bothmer, R. C. Colaninno, C. E. DeForest, B. Gallagher, J. R. Hall, P. Hess, A. K. Higginson, C. M. Korendyke, A. Kouloumvakos, et al., “Near-Sun observations of an F-corona decrease and K-corona fine structure,” *Nature* 576 (Dec., 2019) 232–236.

R. C. Colaninno and A. Vourlidas, “Using Multiple-viewpoint Observations to Determine the Interaction of Three Coronal Mass Ejections Observed on 2012 March 5,” *ApJ* 815 (Dec., 2015) 70-82.

R. C. Colaninno and R. A. Howard, “Update of the Photometric Calibration of the LASCO-C2 Coronagraph Using Stars,” *S. Phys.* 290 (Mar., 2015) 997–1009.

R. C. Colaninno and A. Vourlidas, “First Determination of the True Mass of Coronal Mass Ejections: A Novel Approach to Using the Two STEREO Viewpoints,” *ApJ* 698 (June, 2009) 852–858.

R. C. Colaninno and A. Vourlidas, “Analysis of the Velocity Field of CMEs Using Optical Flow Methods,” *ApJ* 652 (Dec., 2006) 1747–1754.

ABSTRACT

Optical flow is one of the fundamental techniques in the field of Computer Vision. Optical flow is the distribution of apparent velocities of movement of brightness pattern in an image. Horn & Schunck 1981 defined a general algorithm for determining optical flow using a simple regularization term to constrain the problem. Implementations such as Lucas & Kanade 1981 and processing techniques such as coarse-to-fine pyramids have been incorporated to improve the robustness of the technique. Optical flow has been applied to LASCO C2 coronal data. However, past applications were limited by the cadence of the observations relative to the scene velocity and the signal to noise ratio. Beyond cadence and image quality, coronal observations have unique challenges due to the diffuse and dynamic nature of space plasma not found in other applications. New observations coming from PUNCH with higher cadence and signal to noise have renewed interest in these powerful tools. When applied to PUNCH images, optical flow would provide large scale solar wind velocities and velocity map of CME in an automated way. We will explore different optical flow techniques to determine which is most promising for the new observations from PUNCH.

REFERENCES

- [1] Horn, B., & Schunck, B. 1981 A.I., 17, 185
- [2] Mémin, E., & Pérez, P. 1998 IEEE Trans. Im. Pro., 7(5), 703
- [3] Thernisien, A. F., Howard, R., & Vourlidas, A. 2006 ApJ, 652, 763
- [4] Colaninno, R., & Vourlidas, A. 2006 ApJ, 652, 1747
- [5] https://cdaw.gsfc.nasa.gov/CME_list/ (https://cdaw.gsfc.nasa.gov/CME_list/)
- [6] <https://vision.middlebury.edu/flow/> (<https://vision.middlebury.edu/flow/>)